ELSEVIER

Contents lists available at ScienceDirect

Science Bulletin

journal homepage: www.elsevier.com/locate/scib



Article

Experimental quantum Hamiltonian identification from measurement time traces

Shi-Yao Hou a,b,c,d, Hang Li b,c,d, Gui-Lu Long b,c,d,*

- a Microsystem & Terahertz Research Center and Institute of Electronic Engineering, China Academy of Engineering Physics, Mianyang 621999, China
- b State Key Laboratory of Low-dimensional Quantum Physics and Department of Physics, Tsinghua University, Beijing 100084, China
- ^cThe Innovative Center of Quantum Matter, Beijing 100084, China
- ^d Tsinghua National Laboratory of Information Science and Technology, Beijing 100084, China

ARTICLE INFO

Article history: Received 14 April 2017 Received in revised form 9 May 2017 Accepted 10 May 2017 Available online 15 May 2017

Keywords:
Quantum information
Hamiltonian identification
Measurement time traces
Experimental realization
Nuclear magnetic resonance

ABSTRACT

Identifying Hamiltonian of a quantum system is of vital importance for quantum information processing. In this article, we realized and benchmarked a quantum Hamiltonian identification algorithm recently proposed (Zhang and Sarovar, 2014). We realized the algorithm on a liquid nuclear magnetic resonance quantum information processor using two types of working media with different forms of Hamiltonian. Our experiment realized the quantum identification algorithm based on free induction decay signals. We also showed how to process data obtained in a practical experiment. We studied the influence of decoherence by numerical simulations. Our experiments and simulations demonstrate that the algorithm is effective and robust.

© 2017 Science China Press. Published by Elsevier B.V. and Science China Press. All rights reserved.

1. Introduction

One critical task in quantum information processing is to characterize a quantum system so that it can be used for tasks, such as quantum teleportation [1,2], quantum cryptography [3,4], quantum computation [5,6], quantum simulation [7–11] and quantum metrology [12,13]. One way of fully characterizing a quantum system is doing quantum state tomography (QST) and quantum processing tomography (QPT) [14–19]. The QPT approach requires an exponential number of experiments, which makes it difficult to be realized for even a small sized quantum system [20–23].

Meanwhile, various methods based on measurement time traces for Hamiltonian identification have been proposed for general quantum systems. Fourier transformation (FT) of only one measurement observable is used for a single qubit Hamiltonian identification [24]. Temporal evolution of concurrence measure of entanglement is employed to identify arbitrary two-qubit Hamiltonian [25]. Hamiltonian identification using dynamical decouplings was proposed [26]. Schemes of estimating the coupling parameters for a complex quantum network based on measurements of a small part of the network were proposed [27,28]. A basic and general quantum system identification framework has been established on how much knowledge that is attainable about a quantum system for a given experimental setup [29]. Very

recently, Zhang and Sarovar [30] proposed an efficient approach (the ZS approach) for identifying arbitrary Hamiltonian quantum dynamics, taking advantage of available prior knowledge of the system.

One typical dynamical system is the nuclear magnetic resonance (NMR) system, which is well described by quantum mechanics. Moreover, its control technology has been well developed during the 50 years since the birth of NMR. These factors make the NMR system an appealing quantum system for sophisticated manipulation. Therefore, NMR systems are widely used for quantum information processing [31,32]. To obtain the information of an NMR system, modern NMR spectrometers acquire the free induction decay (FID) signals, which are the measurement time traces of certain observables. Schemes based on FT (e.g. FT-NMR) of the FID signals, which is one of the most robust ways of processing FID, have been developed [33,34]. Because the ZS approach is based on measurement time traces for an arbitrary quantum system, the NMR spectrometer provides a practical and controllable system for demonstrating and benchmarking the ZS approach.

In this article, we implemented the ZS approach on an NMR quantum information processor and compared the result with that of FT approach. The experiments were performed with two types of working media with different Hamiltonian forms. Because of different Hamiltonian forms, we have to choose different measurement observables which require distinct experimental setups. Unlike works of NMR quantum computing in last two decades,

^{*} Corresponding author.

E-mail address: gllong@tsinghua.edu.cn (G.-L. Long).

we started from the thermal equilibrium state rather than the pseudo-pure state, and directly processed the FID signals. Our experiments demonstrated that the ZS is an very efficient approach for Hamiltonian identification. We also analysed the influences of imperfect experiment conditions and decoherence on the results using numerical simulations.

2. Algorithm

Here we briefly describe the ZS approach. Suppose now we have an n-qubit quantum system with Hamiltonian \widehat{H} . With the initial state $\rho(0)$, the system evolves, governed by the Hamiltonian \widehat{H} . During the evolution, the expectation value of an observable O at time t is measured and recorded as $\mathbf{y}(t)$. $\mathbf{y}(t)$ is also called the measurement time trace of observable O. The Hamiltonian can be written in a parametrized form,

$$\widehat{H} = \sum_{m} a_m X_m,\tag{1}$$

where a_m is the unknown parameters to be acquired, $X_m \in S = \{X_k | X_k = \sigma_\alpha \otimes \sigma_\beta \otimes \cdots \otimes \sigma_\gamma, \text{ and } X_k \neq I\}$, and $\sigma_\alpha, \sigma_\beta$ and σ_γ are the Pauli matrices σ_x, σ_y and σ_z and σ_z and σ_z identity operator σ_z . The number of the elements in σ_z is σ_z in σ_z . However, if taken into consideration of a practical physical system, the number of the non-zero σ_z can be significantly decreased.

All the elements in set S are Hermitian operators. However, because of the physical constraints, only some of them can be easily measured, e.g., only the transverse magnetization in NMR, denoted by operator σ_x (σ_y), can be observed. The temporal record of the expectations of such an observable O can be collected, which is called a measurement time trace, and denoted by $\mathbf{y}(t)$, then $\mathbf{y}(t) = \text{Tr}\{O\rho(t)\}$, with $\rho(t)$ being the density matrix at time t. Let $\mathbf{y}(t)$ be treated as an output of a linear system, and if we can find a set of $[\mathbf{C}_0, \mathbf{A}_0, \mathbf{x}_0(0)]$, which satisfies $\mathbf{y}(t) = \mathbf{C}_0 \mathbf{e}^{\mathbf{A}_0 t} \mathbf{x}_0(0)$, we call this set a *realization*. For a certain output, various realizations can be obtained. Among these realizations, an invariant function, called *transfer function* Y(s) exists, which is actually the Laplace transformation of the output, i.e.

$$Y(s) = \mathcal{L}(\mathbf{y}(t)) = \mathbf{C}_0(s\mathbf{I} - \mathbf{A}_0)^{-1}\mathbf{x}_0(0), \tag{2}$$

where s is Laplace variable, \mathcal{L} denotes Laplace transformation, and \mathbf{I} is the density matrix with the same dimension of \mathbf{A}_0 . The basic idea of the ZS approach is to find two realizations, one with all the unknown parameters a_m (called realization 1, denoted by $[\mathbf{C}, \widetilde{\mathbf{A}}, \mathbf{x}_a(0)]$) and the other (called realization 2, denoted by $[\widehat{\mathbf{C}}, \widehat{\mathbf{A}}, \widehat{\mathbf{x}}(0)]$) with completely known numbers. With these two realizations, the coefficients of the Laplace variable s can be compared, hence the unknown parameters can be obtained, s i.e.,

$$\mathbf{C}(s\mathbf{I} - \widetilde{\mathbf{A}})^{-1}\mathbf{x}_{a}(0) = \widehat{\mathbf{C}}(s\mathbf{I} - \widehat{\mathbf{A}})^{-1}\hat{\mathbf{x}}(0). \tag{3}$$

A schematic of the ZS approach is shown in Fig. 1.

Realization 1 is obtained from the parametrized Hamiltonian \widehat{H} , the observable O and the initial state $\rho(0)$. The observable and the initial state are appropriately chosen artificially according to the structure of a physical system. In such case, the vector $\mathbf{x}_a(0)$ describes the initial system state $\rho(0)$, the matrix $\widetilde{\mathbf{A}}$ describes the dynamical evolution driven by \widehat{H} , and the matrix \mathbf{C} predicts the measurement outcome $\mathbf{y}(t)$ for the system state \mathbf{x}_t .

Realization 2 is obtained solely by performing numerical methods, without relying on specific knowledge of the underlying system. One way to do so is the eigenstate realization algorithm (ERA) [35]. Technical details on how to obtain the two realizations is out of the scope of this article and shown in the Electronic Supplementary Material.

3. Experiments setup and results

The ZS approach was tested in a two-qubit and a three-qubit NMR system, which were implemented with ¹³C-labelled trichlor-oethylene (TCE) and ¹³C-labelled L-alanine (ALA) as the working media, respectively. The molecular structures and the thermal spectra of ALA and TCE are shown in Fig. 2.

The Hamiltonian of a liquid NMR system is $(\hbar = 1)$

$$\widehat{H}_{\text{NMR}} = \sum_{i=1}^{N} \pi \nu_{i} \sigma_{z}^{j} + \sum_{i>i=1}^{N} \frac{\pi J_{ij}}{2} \boldsymbol{\sigma}^{i} \cdot \boldsymbol{\sigma}^{j}, \tag{4}$$

where $2\pi v_i$ is the Larmor frequency for the ith spin, J_{ij} is the indirect coupling constant between the ith and jth spin. In weak coupling, $|v_i-v_j|\gg |J_{ij}|$, which is valid for ALA, only the secular components of the scalar coupling survive. Hence the Hamiltonian of ALA is parametrized as

$$\widehat{H}_{ALA} = a_1^A \sigma_z^1 + a_2^A \sigma_z^2 + a_3^A \sigma_z^3 + a_4^A \sigma_z^1 \sigma_z^2 + a_5^A \sigma_z^1 \sigma_z^3 + a_6^A \sigma_z^2 \sigma_z^3.$$
 (5)

TCE is strongly coupled, and its parametrized Hamiltonian has a more complicated form,

$$\widehat{H}_{TCE} = a_1^T \sigma_z^1 + a_2^T \sigma_z^2 + a_3^T (\sigma_y^1 \sigma_y^2 + \sigma_y^1 \sigma_y^2 + \sigma_z^1 \sigma_z^2).$$
 (6)

Once the Hamiltonian is parametrized, the observable can be decided. For TCE, $O^{\rm T}=\sigma_{\rm x}^2$ is chosen, and one qubit time trace is sufficient to identify the whole Hamiltonian because of strong coupling. Whereas for ALA, $O^{\rm A}=\sigma_{\rm x}^1+\sigma_{\rm x}^2+\sigma_{\rm x}^3$ has to be chosen as the observable because of the nature of the weak coupling Hamiltonian.

Then we prepare the initial states. Different forms of Hamiltonian require different experimental strategies. Different from NMR quantum computing with pseudo-pure initial state [31], Hamiltonian characterization should start directly from states that are easily prepared without knowing the Hamiltonian details, e.g., state $\rho(0) = \sum_j \sigma_x^j$. For ALA, we repeated the experiments for three times with three different initial states σ_x^1, σ_x^2 , and σ_x^3 , each corresponds to a different $\mathbf{x}_a(0)$ for ALA. Choosing three initial states instead of one simplifies the data processing procedure. For TCE, a single input state σ_x^2 is enough.

After preparation, $\rho(0)$ starts to evolve under the system Hamiltonian, hence the macroscopic magnetization in NMR rotates. The rotation of the magnetization induces an electromagnetic wave which is received by a coil, and the signal received is called the free induction decay(FID) signal. The FID signal acquired by modern NMR spectrometers contains real and imaginary parts. The real part is

$$V_R(t) = \alpha \text{Tr}\{F_x \rho(t)\},\tag{7}$$

where α is a coefficient related to the spectrometer, $\rho(t)$ is the density matrix of the system at time t, and $F_x = \sum_j \sigma_x^j$, where the summation includes the spins in the chosen observable. For TCE, only the second spin is observed and for ALA, all three qubits are observed. Thus the observable for TCE is $F_x^{\rm T} = \sigma_x^2$ and for ALA is $F_x^{\rm A} = \sigma_x^1 + \sigma_x^2 + \sigma_x^3$, which are exactly the observables we chose for ZS approach. The state $\rho(t)$ evolves as $\rho(t) = U \rho(0) U^{\dagger}$ with $U = \exp(-i \hat{H}_{\rm NMR} t)$. From this discussion, we can see that the real

¹ Detailed information is given in the Electronic Supplementary Material, which also includes the details of the experiment and numerical simulations.

² Theoretically, the equation $\mathbf{y}(t) = \mathbf{C}\mathbf{e}^{\widetilde{\mathbf{A}}t}\mathbf{x}_a(0)$ can be solved to obtain all the unknown parameters in $\widetilde{\mathbf{A}}$. However, the right hand side of this equation is a transcendental function of a_m 's, which makes it infeasible obtaining a_m 's.

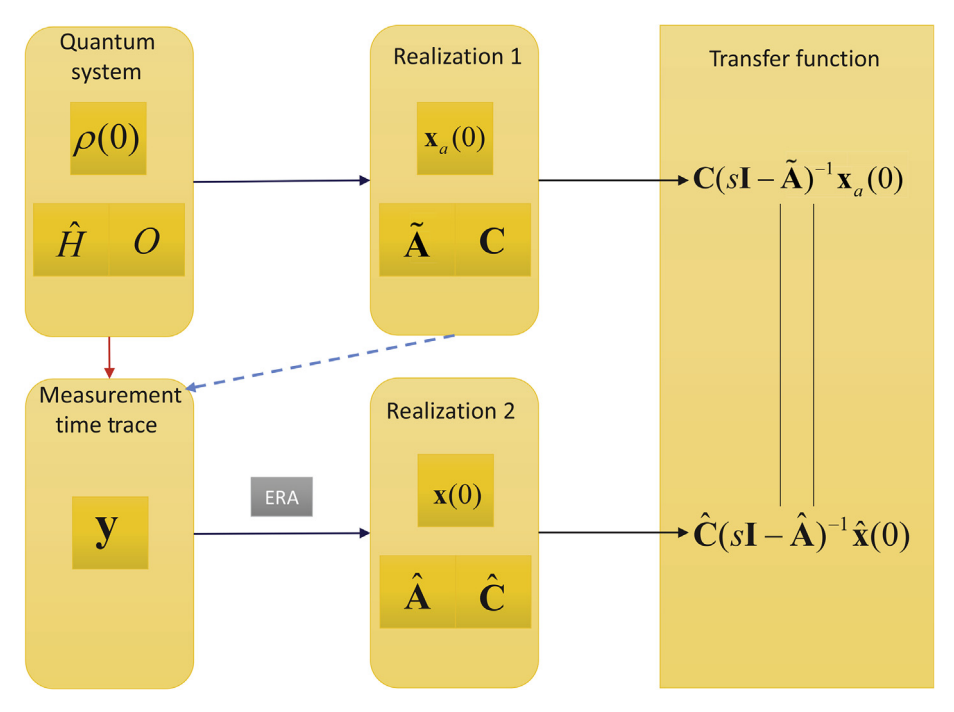


Fig. 1. (Color online) Schematic of the ZS approach. From the forms of density matrix, Hamiltonian and observable, realization 1 ($[\mathbf{C}, \bar{\mathbf{A}}, \mathbf{x}_a(0)]$) with the unknown parameters can be obtained. From the measurement time traces, realization 2 ($[\hat{\mathbf{C}}, \bar{\mathbf{A}}, \mathbf{x}(0)]$) can be obtained. From realizations, transfer functions could be obtained, which is unique for a certain physical system. Therefore, by solving the equation of equalizing the two transfer functions obtained from two realizations, we can get the unknown parameters.

part of FID is the measurement time traces required by the ZS approach.

After the FID signals are acquired, one can obtain a realization through ERA. However, data processing is not that simple due to the imperfections of a spectrometer. We have to deal with two problems, the dead time of the spectrometer and the unknown coefficient α . The dead time problem can be solved by doing phase correction on a spectrometer, and the unknown coefficient problem can be solved by scaling the FID properly. Detailed discussion about processing the experimental data before ERA is shown in the Electronic Supplementary Material.

Then ERA is performed to obtain a realization of the system on the processed FID signal. In our experiments and numerical simulations, 1600 points were used in ERA. Compared with the number of points (more than 16,000 in our experiments) FT-NMR utilized, the number of the points ERA used is quite small. Once the realization is obtained, the transfer function can be calculated. By comparing the transfer functions, the parameters of the Hamiltonian are obtained. The results of the Hamiltonians of TCE and ALA are shown in Tables 1 and 2, respectively.

From Tables 1 and 2, we can see that the parameters obtained from FT and that from the ZS approach agree well with each other. The absolute difference between the experimental values and theoretical values of the chemical shifts for TCE is about 1 Hz (note there is a multiplication of π between the chemical shift and the parameters a_j), which is only slightly larger than 0.5 Hz, the resolution of a modern FT-NMR spectrometer. The relative errors for the parameters related to the chemical shifts of ALA $(a_1^{\rm A}-a_3^{\rm A})$ are smaller than that of TCE $(a_1^{\rm T},a_2^{\rm T})$, while at the same time, the relative errors for the parameters related to the spin-spin couplings of ALA $(a_4^{\rm A},a_6^{\rm A})$ are larger than that of TCE $(a_3^{\rm T})$. From these comparisons, we can say that the larger the value of a parameter, the more robust of the result. Despite the small relative error, the absolute differences of the chemical shifts of ALA are about 2-4 Hz, which is tiny but can be identified on modern NMR spectrometers. The

extremely weak coupling can not be identified through looking at the whole spectrum (which means the observable is $\sigma_x^1 + \sigma_x^2 + \sigma_x^3$), both by using FT and the ZS approach. This is caused by the low resolution of a spectrum with a large spectral width (SW) and the decoherence time T_2 . SW is a parameter decided before acquisition. Since the difference between the chemical shifts of C1 and C3 of alanine is large, to obtain the whole spectrum, the spectral width in Hz (SWH) has to be very large. The FID resolution in Hertz is FIDRES=SWH/TD.3 As FIDRES is proportional to SWH, a large SWH means a large FIDRES, hence low resolution. Combined with the line broadening caused by decoherence, the weak coupling can not be identified on the spectrum of FT-NMR, which means that the information of J_{13} is lost during the acquisition. To identify weak couplings, a small SWH (for ALA, it can be set to less than 100 Hz) should be chosen and the transmitter frequency should be set to the frequency of C1 or C3.

It is worth noting that only the absolute value of the parameters is provided in the Tables 1 and 2. For a signal $V(t) = \cos(\omega t)$, the result of FT will give frequencies ω and $-\omega$. Therefore, to identify the sign of chemical shifts, modern NMR spectrometers use quadrature detection [34], where the imaginary FID is generated and employed to assist identifying the frequencies, while during our experiments with the ZS approach, only F_x is observed. The signs of the spin-spin couplings can not be identified by just obtaining the 1D spectrum. To identify these signs, additional experiments such as COSY-45 or spin polarization transfer are required. From the above discussion, we can see that the ZS approach gives almost the same amount of information as that provided by FT.

Besides FT, other methods, such as maximum entropy method [36,37], linear prediction [38,39] are also in common use. Though not as robust as FT, these methods have advantages in certain cases

³ See Bruker manuals of Topspin for details.

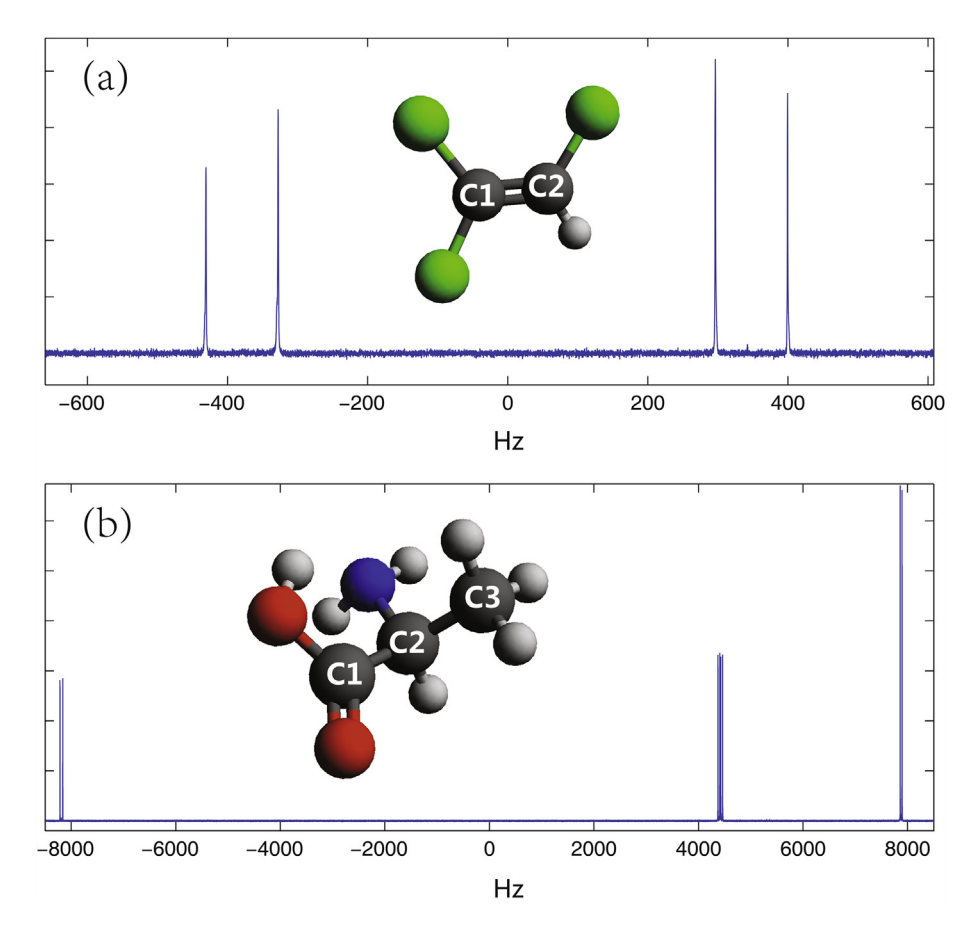


Fig. 2. (Color online) Molecule structure and spectrum for TCE (a) and ALA (b). The gray balls represent ¹³C. Both spectra are obtained with hydrogen decoupled. The difference in the heights of the peaks in TCE carbon spectra are caused by strong coupling between the two carbons.

 Table 1

 Experimental results for TCE. Relative error is defined as |FT result-ZS result|/FT result. The values of the parameters in FT result are obtained by numerically fitting the Fourier transformed spectra.

a_m	X_m	FT result	ZS result	Relative error
a_1	σ_z^1	1180.6	1179.4	1.05×10^{-3}
a_2	σ_z^2	1081.2	1082.5	1.25×10^{-3}
a_3	$\sigma_x^1\sigma_x^2+\sigma_y^1\sigma_y^2+\sigma_z^1\sigma_z^2$	161.9	162.6	4.24×10^{-3}

Table 2Experimental results for ALA. Relative error is defined as |FT result–ZS result||FT result. The values of the parameters in FT result are obtained by numerically fitting the Fourier transformed spectra.

a_m	X_m	FT result	ZS result	Relative error	
a_1	σ_z^1	25723.3	25721.2	7.98×10^{-6}	
a_2	σ_z^2	13876.7	13881.5	3.44×10^{-4}	
a_3	σ_z^3	24745.6	24749.9	1.71×10^{-4}	
a_4	$\sigma_z^1\sigma_z^2$	84.8	84.3	5.5×10^{-3}	
a_6	$\sigma_z^2 \sigma_z^3$	54.8	55.7	1.59×10^{-2}	

such as when there are only a few data points. Since the data points used by the ZS approach is much smaller than that used by FT, our experiments show that the ZS approach is also applicable in such cases.

4. Decoherence

In NMR systems, decoherence is a common feature, which causes error in the ZS approach and leads information loss of

parameter $a_5^{\rm A}$. For practical experiments, the decoherence parameters are decided according to the spectrometer and the preparation of the sample. Therefore, to benchmark the ZS approach with the presence of decoherence, numerical simulations are employed. One common parameter used to characterize decoherence is T_2 . ⁴

⁴ In this article, all T_2 is actually T_2^* . T_2^* consists of T_2 and the inhomogeneity of the magnetic field. The inhomogeneity can be refocused by pulses. But when we acquire the FID, the inhomogeneity always exists and can not be eliminated. Thus all the T_2 's described in this article is T_2^* , which can be straightly obtained by fitting the spectra.

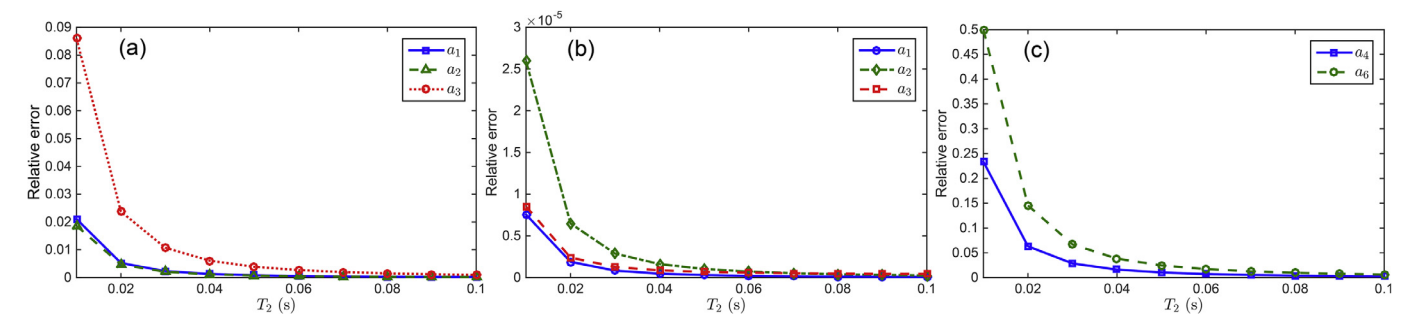


Fig. 3. (Color online) Relative error against T_2 . (a) The three parameters for TCE. (b) The three parameters related to Larmor frequency of ALA. (c) The two parameters related to the two largest coupling of ALA.

Numerical simulations are performed to benchmark the influence of T_2 . Using the T_2 model presented in Ref. [33], the output FID reads

$$V_{\rm Rd}(t) = \alpha \sum_{\bf r} F_{\rm XrS} \rho_{\rm sr}({\bf 0}) e^{(i\omega_{\rm rs} - \lambda_{\rm rs})t}, \tag{8}$$

where F_{xrs} ($\rho_{sr}(0)$) denotes the r- and s-th (s- and r-th) entry of $F_x(\rho(0))$, ω_{rs} denotes the frequency between energy level r ans s and λ_{rs} is the relaxation rate, i.e., $\omega_{rs} = \langle r|\hat{H}_{\text{NMR}}|r\rangle - \langle s|\hat{H}_{\text{NMR}}|s\rangle$ and $\lambda_{rs} = 1/T_2^{rs}$. For simplicity and without loss of generosity, let all the spins relax at the same rate, so $T_2^{rs} = T_2$ and $V_d(t) = V(t) \exp\{-t/T_2\}$. Our simulations show that, the magnitudes of the absolute value of the parameters in Hamiltonian decide the sensitivity to T_2 . The parameters with smaller values are more sensitive than that with larger values, as shown in Fig. 3.

In our simulations, the T_2 's are chosen to be from 0.01 to 0.1 s, which are shorter than T_2 of the systems. The couplings of ALA's are much smaller than that of TCE's, hence the errors brought by T_2 to the couplings of ALA's are much larger than that of TCE's, while on the contrary, the value of the chemical shifts of ALA's are much larger than that of TCE's, so the relative errors for the chemical shifts are smaller for ALA than that for TCE. It is reasonable to find out that the longer the T_2 , the smaller the relative errors. Here, the coupling J_{13} is not plotted, since for short T_2 , it can not be identified. In classical FT-NMR, T_2 broadens the peak width by $1/(\pi T_2)$, which is about 3 Hz when $T_2 = 0.1$ s. The extremely weak coupling is about 1.8 Hz, thus the information of J_{13} is lost during the acquisition due to short T_2 . According to our simulation, if the T_2 time is greater than 1.5 s, J_{13} can be obtained with relative error smaller than 0.02 using the ZS approach.

5. Discussion and conclusions

The number of the parameters a_m 's of \widehat{H} in Eq. (1) is 4^n-1 , which is exponential, making QPT extremely hard to be performed. If without any prior knowledge of the system, all these a_m 's have to be identified using the ZS approach, which means the scale of the problem grows exponentially and the ZS approach is hardly scalable. However, because of the physical constraints on system energy, locality and structure, the number of the non-zero a_m 's would decrease rapidly, which significantly simplifies the problem. Taking the liquid NMR system Hamiltonian of Eq. (4) with weak coupling as an example, the number of the non-zero a_m 's is $O(n^2)$, which is polynomial, and can be further reduced because the indirect spin-spin coupling hardly exists between two spins that are four chemical bonds away. From this point of view, the ZS approach for the liquid NMR Hamiltonians⁵ is scalable as the number of qubits grows.

In summary, we have realized the ZS approach using an NMR quantum information processor with different work media. We showed that by choosing suitable observables for a given form of coupling, weak or strong coupling, the Hamiltonian can be efficiently identified using the ZS approach. Our experiments show that the ZS approach simplifies for the strong coupling systems, thus it can be used to identify these systems, such as solid-state and liquid crystal NMR systems, whose Hamiltonians are difficult to identify using FT approach. We also studied the influence of T_2 on the result of the ZS approach. The numerical simulation indicated that a very short T_2 , implying a strong decoherence, can downgrade the ZS approach. However for a reasonable T_2 , the ZS approach is efficient and robust.

Conflict of interest

The authors declare that they have no conflict of interest.

Acknowledgments

This work was supported by the National Natural Science Foundation of China (11175094 and 91221205), the National Basic Research Program of China (2011CB9216002). The authors would like to thank J. Zhang and M. Sarovar for helpful discussions, and IQC, University of Waterloo, for providing the software package for NMR experiment simulation.

Appendix A. Supplementary data

Supplementary data associated with this article can be found, in the online version, at http://dx.doi.org/10.1016/j.scib.2017.05.013.

References

- [1] Bennett CH, Brassard G, Crépeau C, et al. Teleporting an unknown quantum state via dual classical and Einstein-Podolsky-Rosen channels. Phys Rev Lett 1993:70:1895-9
- [2] Li TC, Yin ZQ. Quantum superposition, entanglement, and state teleportation of a microorganism on an electromechanical oscillator. Sci Bull 2016;61:163–71.
- [3] Bennett CH, Brassard G, et al. Quantum cryptography: Public key distribution and coin tossing. Proceedings of IEEE International Conference on Computers, Systems and Signal Processing, vol. 175. New York.
- [4] Long GL, Liu XS. Theoretically efficient high-capacity quantum-keydistribution scheme. Phys Rev A 2002;65:032302.
- [5] Knill E, Laflamme R, Milburn GJ. A scheme for efficient quantum computation with linear optics. Nature 2001;409:46–52.
- [6] Bassett LC, Awschalom DD. Quantum computation: spinning towards scalable circuits. Nature 2012;489:505–7.
- [7] Georgescu IM, Ashhab S, Nori F. Quantum simulation. Rev Mod Phys 2014:86:153–85.
- [8] Lu Y, Feng GR, Li YS, et al. Experimental digital quantum simulation of temporal-spatial dynamics of interacting fermion system. Sci Bull 2015;60:241–8.
- [9] Pearson J, Feng G, Zheng C, et al. Experimental quantum simulation of avian compass in a nuclear magnetic resonance system. Sci China Phys Mech Astron 2016;59:120312.

 $[\]overline{\ }^5$ The number of non-zero a_m 's for strong coupling system is $(3 \times n^2 - n)/2$, which is also polynomial.

- [10] Liu Y, Zhang FH. First experimental demonstration of an exact quantum search algorithm in nuclear magnetic resonance system. Sci China Phys Mech Astron 2015;58:070301.
- [11] Jin FZ, Chen HW, Rong X, et al. Experimental simulation of the unruh effect on an nmr quantum simulator. Sci China Phys Mech Astron 2016;59:630302.
- [12] Giovannetti V, Lloyd S, Maccone L. Quantum metrology. Phys Rev Lett 2006;96:010401.
- [13] Liu Y, Kong F, Shi F, et al. Detection of radio-frequency field with a single spin in diamond. Sci Bull 2016;61:1132–7.
- [14] Wang HY, Zheng WQ, Yu NK, et al. Quantum state and process tomography via adaptive measurements. Sci China Phys Mech Astron 2016;59:100313.
- [15] Fei SM. Adaptive-measurement based quantum tomography. Sci China Phys Mech Astron 2016;60:020331.
- [16] Zhou T. Quantum measurement in coherence-vector representation. Sci China Phys Mech Astron 2016;59:640301.
- [17] Li W, Jin YB, Yu XD. Characterization of squeezed states with controllable coherent light injection at sidebands. Sci China Phys Mech Astron 2017;60:050321.
- [18] Chen J, Guo C, Ji Z, et al. Joint product numerical range and geometry of reduced density matrices. Sci China Phys Mech Astron 2016;60:020312.
- [19] Qin Z, Prasad AS, Brannan T, et al. Complete temporal characterization of a single photon. Light Sci Appl 2015;4:e298.
- [20] Poyatos JF, Cirac JI, Zoller P. Complete characterization of a quantum process: the two-bit quantum gate. Phys Rev Lett 1997;78:390–3.
- [21] Chuang IL, Nielsen MA. Prescription for experimental determination of the dynamics of a quantum black box. J Mod Opt 1997;44:2455–67.
- [22] Mohseni M, Rezakhani AT, Lidar DA. Quantum-process tomography: resource analysis of different strategies. Phys Rev A 2008;77:032322.
- [23] Feng G, Xu G, Long GL. Experimental realization of nonadiabatic holonomic quantum computation. Phys Rev Lett 2013;110:190501.
- [24] Cole JH, Schirmer SG, Greentree AD, et al. Identifying an experimental twostate hamiltonian to arbitrary accuracy. Phys Rev A 2005;71:062312.

- [25] Devitt SJ, Cole JH, Hollenberg LCL. Scheme for direct measurement of a general two-qubit hamiltonian. Phys Rev A 2006;73:052317.
- [26] Wang ST, Deng DL, Duan LM. Hamiltonian tomography for quantum many-body systems with arbitrary couplings. New J Phys 2015;17:093017.
- [27] Burgarth D, Maruyama K, Nori F. Coupling strength estimation for spin chains despite restricted access. Phys Rev A 2009;79:020305.
- [28] Burgarth D, Maruyama K. Indirect hamiltonian identification through a small gateway. New J Phys 2009;11:103019.
- [29] Burgarth D, Yuasa K. Quantum system identification. Phys Rev Lett 2012;108:080502.
- [30] Zhang J, Sarovar M. Quantum hamiltonian identification from measurement time traces. Phys Rev Lett 2014;113:080401.
- [31] Vandersypen LMK, Chuang IL. NMR techniques for quantum control and computation. Rev Mod Phys 2005;76:1037–69.
- [32] Ryan CA, Negrevergne C, Laforest M, et al. Liquid-state nuclear magnetic resonance as a testbed for developing quantum control methods. Phys Rev A 2008;78:012328.
- [33] Ernst RR, Bodenhausen G, Wokaun A. Principles of nuclear magnetic resonance in one and two dimensions. Oxford: Clarendon Press; 1987.
- [34] Levitt MH. Spin dynamics: basics of nuclear magnetic resonance. John Wiley & Sons; 2008.
- [35] Juang JN, Pappa RS. An eigensystem realization algorithm for modal parameter identification and model reduction. J Guid Control Dyn 1985;8:620–7.
- [36] Hore P. NMR data processing using the maximum entropy method. J Magn Reson 1985;62:561–7.
- [37] Sibisi S, Skilling J, Brereton RG, et al. Maximum entropy signal processing in practical nmr spectroscopy. Nature 1984;311:446–7.
- practical nmr spectroscopy, Nature 1984;311:440–7.

 [38] Led JJ, Gesmar H. Application of the linear prediction method to NMR spectroscopy. Chem Rev 1991;91:1413–26.
- [39] Stephenson DS. Linear prediction and maximum entropy methods in nmr spectroscopy. Prog Nucl Magn Reson Spectrosc 1988;20:515–626.